ADVANCED FUNCTIONAL MATERIALS
www.afm-journal.de

Facile Generation of $L1_0$-FePt Nanodot Arrays from a Nanopatterned Metallopolymer Blend of Iron and Platinum Homopolymers

Qingchen Dong, Guijun Li, Cheuk-Lam Ho, Chi-Wah Leung, Philip Wing-Tat Pong,* Ian Manners,* and Wai-Yeung Wong**

Hard ferromagnetic ($L1_0$ phase) FePt alloy nanoparticles (NPs) with extremely high magnetocrystalline anisotropy are considered to be one of the most promising candidates for the next generation of ultrahigh-density data storage system. The question of how to generate ordered patterns of $L1_0$-FePt NPs and how to transform the technology for practical applications represents a key current challenge. Here the direct synthesis of $L1_0$ phase FePt NPs by pyrolysis of Fe-containing and Pt-containing metallopolymer blend without post-annealing treatment is reported. Rapid single-step fabrication of large-area nanodot arrays (periodicity of 500 nm) of $L1_0$-ordered FePt NPs can also be achieved by employing the metallopolymer blend, which possesses excellent solubility in most organic solvents and good solution processability, as the precursor through nanoimprint lithography (NIL). Magnetic force microscopy (MFM) imaging of the nanodot pattern indicates that the patterned $L1_0$ phase FePt NPs are capable of exhibiting decent magnetic response, which suggests a great potential to be utilized directly in the fabrication of bit patterned media (BPM) for the next generation of magnetic recording technology.

1. Introduction

Chemically ordered $L1_0$ phase FePt nanoparticles (NPs) have attracted growing interest owing to their high magnetocrystalline anisotropy $K_u \approx 7 \times 10^6$ J m^{-3} in the bulk phase and high chemical stability which allows its great potential for future ultrahigh density magnetic data recording.[1] Typical synthetic methods for the generation of $L1_0$ phase FePt NPs usually involve two steps: firstly, the separated Fe- and Pt-sources, which are usually inorganic chemical reagents, are mixed up and allowed to react in a high-boiling organic solvent to give rise to superparamagnetic A_1 phase FePt NPs. Then, the resulting A_1 FePt NPs undergo a post-annealing treatment to transform the superparamagnetic A_1 phase to the desired ferromagnetic $L1_0$ phase. However, undesirable problems such as agglomeration, sintering and broad particle size distribution are concomitant with this method.[2–4] Although the use of several FePt-containing organometallic complexes as single-source precursors to directly synthesize $L1_0$ phase FePt has been explored,[5–7] this is unfavorable for future data storage devices as the patterning of the resulting $L1_0$-FePt NPs is very challenging. As far as the patterning techniques are concerned, traditional lithographic patterning methods such as electron-beam lithography (EBL) and UV photolithography (UVL) are not well-suited for mass

Dr. Q. C. Dong
Key Laboratory of Interface Science and Engineering in Advanced Materials
Ministry of Education
Taiyuan, 030024, PR China
Dr. Q. C. Dong
Research Center of Advanced Materials Science and Technology
Taiyuan University of Technology
Taiyuan, 030024, PR China
Dr. Q. C. Dong, Dr. C.-L. Ho, Prof. W.-Y. Wong
Institute of Molecular Functional Materials
Department of Chemistry and Institute of Advanced Materials
Hong Kong Baptist University
Waterloo, Road, Hong, Kong, PR China
E-mail: rwywong@hkbu.edu.hk
Prof. W.-Y. Wong, Dr. C.-L. Ho
HKBU Institute of Research and Continuing Education
Shenzhen Virtual University Park
Shenzhen, 518057, China, PR China
G. J. Li, Prof. P. W.-T. Pong
Department of Electrical and Electronic Engineering
The University of Hong Kong
Pokfulam Road, Hong Kong, PR China
E-mail: ppong@eee.hku.hk
Prof. C.-W. Leung
Department of Applied Physics
Hong Kong Polytechnic University
Hung Hom, Hong Kong, PR China
E-mail: dennis.leung@polyu.edu.hk
Prof. Ian Manners
School of Chemistry
University of Bristol
Bristol, BS8, 1TS, UK
E-mail: ian.manners@bristol.ac.uk

DOI: 10.1002/adfm.201301143

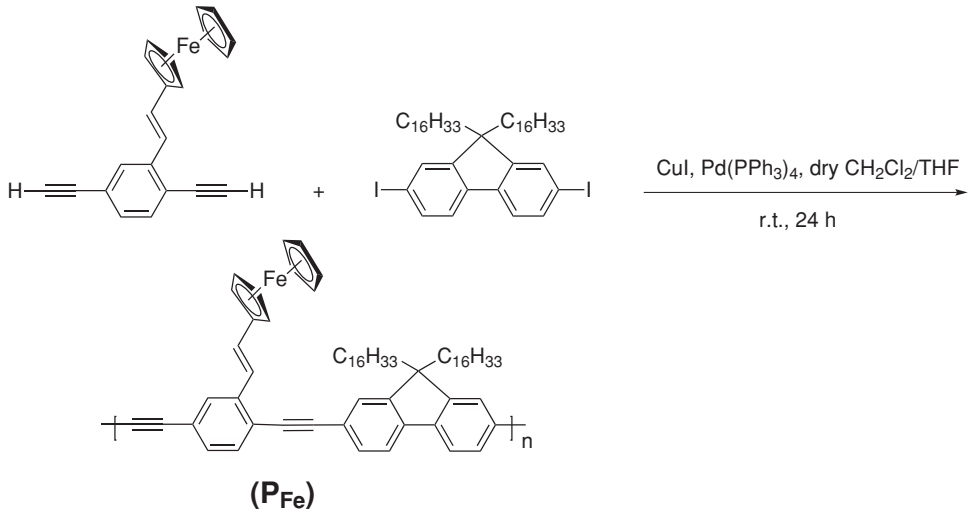

Scheme 1. Synthetic route of Fe-containing metallopolymer ($\mathbf{P}_{Fe}$).

production due to the limitations such as high start-up cost, complex procedures, light diffraction limits or beam scattering, etc.[8,9] Nanoimprint lithography (NIL) has attracted growing interest in the last decade owing to its characteristics of high throughput with high resolution, low cost and simple operation which allows for mass production. Theoretically, NIL can offer a resolution of patterning sub-5 nm features over very large areas which is indeed desirable for industrial fabrication of bit patterned media (BPM).[10]

In recent years, metallopolymers have been utilized for the synthesis of metal NPs with desired structures, narrow size distributions, precisely controllable compositions and areal densities.[11–13] Additionally, owing to the key advantage of the film-forming capability of metallopolymer, patterned metal NPs can be achieved conveniently over large areas on various substrates by pyrolysis or photolysis of the patterned metallopolymer through NIL; such work is important for many applications based on metal nanostructures.[11,14,15] More recently, by taking the advantage of the film-forming property of a polyferroplatinyne metallopolymer with excellent solubility in common organic solvents, our group has reported a new method for the direct fabrication of $L1_0$ phase FePt alloy NPs combined with the unparalleled advantage of direct patterning of ferromagnetic NPs through NIL, which can serve as $L1_0$-FePt-type BPM for future high-density perpendicular magnetic data recording.[16]

Although the access to a wide variety of metallopolymers has been developed in the past several decades owing to the exploration of various synthetic approaches, polymerization processes and starting materials,[17–19] it is still difficult to incorporate two different metal centers into the backbone of the metallopolymers.[20] Meanwhile, most of the heterobimetallic metallopolymers exhibit poor solubility in common organic solvents, which limits their practical application in patterned metal nanostructured media in a large scale and over large areas.[12] Therefore, we report here the synthesis of two mononuclear metallopolymers (viz., Fe-containing metallopolymer and Pt-containing metallopolymer), which typically exhibit excellent solubility in common organic solvents and are readily synthesized in comparison to binary-metal-containing metallopolymers. Furthermore, by blending the Fe-containing metallopolymer and Pt-containing metallopolymer with equiatomic ratio of Fe and Pt and the pyrolysis of the resulting polymer blend, $L1_0$ phase FePt alloy NPs with an average size of 4.9 nm and a narrow size distribution were synthesized directly. Moreover, patterned nanodot arrays of $L1_0$-FePt NPs were also achieved through the pyrolysis of the corresponding nanopatterned polymer blend fabricated using NIL technique.

2. Results and Discussions

2.1. Synthesis and Characterization of Fe-containing and Pt-containing Metallopolymers

Scheme 1 and **Scheme 2** show the chemical structures and synthetic routes of the Fe-containing metallopolymer (denoted as $\mathbf{P}_{Fe}$) and Pt-containing metallopolymer (denoted as $\mathbf{P}_{Pt}$), respectively (detailed synthetic procedures for the ligands can be found in the Supporting Information). $\mathbf{P}_{Fe}$ was synthesized from a diiodofluorene compound and a ferrocene-anchored diethynyl ligand, which undergo a well-known Sonogashira coupling reaction. $\mathbf{P}_{Pt}$ was synthesized from a diethynylfluorene ligand and a platinum(II)-diimine dichloride complex through the copper(I)-catalyzed dehydrohalogenation process. All these polymerization reactions proceeded with satisfisfactory yields to afford the two homopolymers $\mathbf{P}_{Fe}$ and $\mathbf{P}_{Pt}$. These metallopolymers were purified by repeated precipitation in a minimum volume of dichloromethane from methanol for 2–3 times to get rid of any inorganic catalysts and the low-molecular-weight species.

These two metallopolymers are air-stable and soluble in common organic solvents, which allow them to be characterized by ^{1}H NMR spectroscopy (see Experimental Section). The peak due to the C≡C stretching vibrational frequency at around 2100 cm^{-1} in the IR spectrum confirmed the existence of C≡C bond in the backbone of $\mathbf{P}_{Fe}$ and $\mathbf{P}_{Pt}$. The thermal stability of $\mathbf{P}_{Fe}$ and $\mathbf{P}_{Pt}$ was examined by thermal gravimetry analysis (TGA)

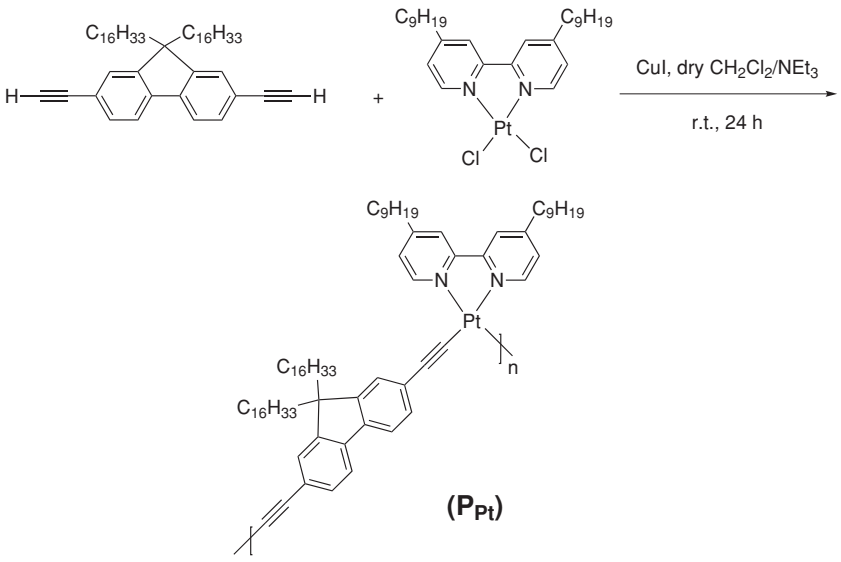

Scheme 2. Synthetic route of Pt-containing metallopolymer ($\mathbf{P}_{Pt}$).

under nitrogen. Analysis of the TGA trace (at a heating rate of 20 °C min^{-1}) shows the onset decomposition temperature of $\mathbf{P}_{Fe}$ and $\mathbf{P}_{Pt}$ to be 321 ± 5 °C and 316 ± 5 °C, respectively.

2.2. Generation and Characterization of $L1_0$ Phase FePt NPs from Controlled Pyrolysis of Metallopolymer Blend

Firstly, $\mathbf{P}_{Fe}$ and $\mathbf{P}_{Pt}$ with equiatomic ratio of Fe and Pt were dissolved in chloroform and the mixture was allowed to sonicate for 1 h to mix them up completely. After that, the organic solvent was evaporated. The resulting fully mixed metallopolymer blend then underwent pyrolytic treatment at 800 °C for 1 h under an argon atmosphere to give rise to FePt NPs.

The composition and structure of as-synthesized FePt NPs were studied by powder X-ray diffraction (PXRD) method (**Figure 1**). The (001) and (110) peaks represent the characteristic peaks of $L1_0$-structured FePt NPs and no peaks due to the Fe and Pt single-element phases in the XRD spectrum can be detected. This manifests the fact that the $L1_0$ phase FePt alloy NPs can be generated directly through pyrolysis of the as-prepared metallopolymer blend without the need of any post-annealing treatment. The reason for this phenomenon can be attributed to the effect of the decomposed organic fractions which acts as both the reducing agent and supporting matrix to facilitate the generation of chemically ordered $L1_0$ or face-centered-tetragonal (fct) phase FePt NPs, which is similar to the mechanism of the intermatrix synthetic approach for the one-step synthesis of fct FePt particles reported recently.[21] Intermatrix synthesis usually requires a chemically and thermally robust supporting matrix such as TiO_2 combined with organic ligands such as acetylacetonate ligands which act as the reducing agent and decomposes to reduce metal ions to the zero valent state.[21] In our case, the decomposed organic fractions serving as the negative radical can reduce the metal ions to zero valence, and during pyrolysis, the organic fractions will be transformed to ceramic carbonaceous matrix to support the accommodation of alloying FePt intermediates.

The morphology of the resulting FePt NPs was studied by transmission electron microscopy (TEM) image. **Figure 2**a shows a TEM image of as-prepared $L1_0$ phase FePt NPs, which are embedded in a carbonaceous matrix. Figure 2b displays the histogram of the size distribution of the resulting FePt NPs through analysis of the TEM image (Figure 2a), indicating that the as-synthesized $L1_0$-FePt alloy particles have an effective average size of 4.9 ± 0.73 nm, as depicted in Figure 2b. This is desirable since the size uniformity of NPs is very important for magnetic recording media in order to achieve a sufficient signal-to-noise ratio in the data readback process.[24] Figures 2c and d are the high-resolution TEM images of a single FePt NP with well-faceted spherical morphology, indicating that the resulting FePt NPs are of high crystallinity. The continuous fringe-patterns with interplanar distances of around 0.221 nm and 0.373 nm, corresponding to (111) and (001) d-spacings for $L1_0$-FePt NPs, can be observed clearly.[22,23] Thus, this further confirms that the structure of the FePt NPs is chemically ordered $L1_0$ phase. The results of energy-dispersive X-ray (EDX) elemental analysis show that the composition of the resulting FePt alloy NPs is Fe-rich with atomic ratio of Fe to Pt to be approximately 59:41.

2.3. Generation and Characterization of Patterned $L1_0$-FePt NPs from Pyrolysis of Nanoimprinted Metallopolymer Blend

According to the above compositional analysis and structural characterization of the NPs as-generated from the pyrolysis of a metallopolymer blend of Fe-containing and Pt-containing

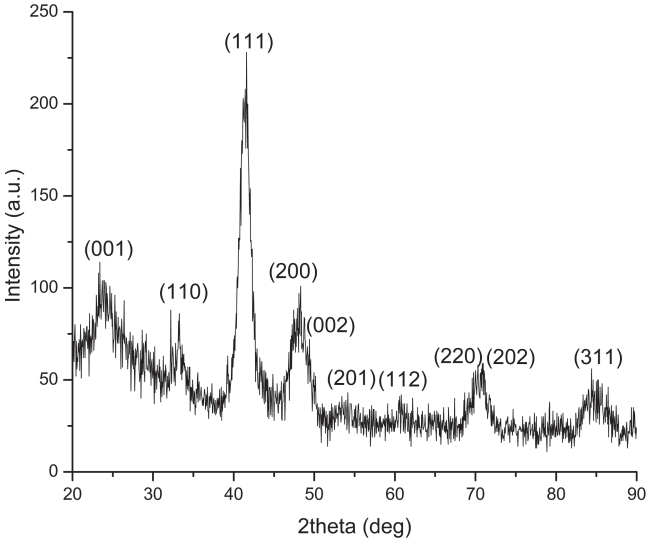

Figure 1. Powder X-ray diffraction (PXRD) spectrum of the FePt NPs synthesized at 800 °C for 1 h under Ar.

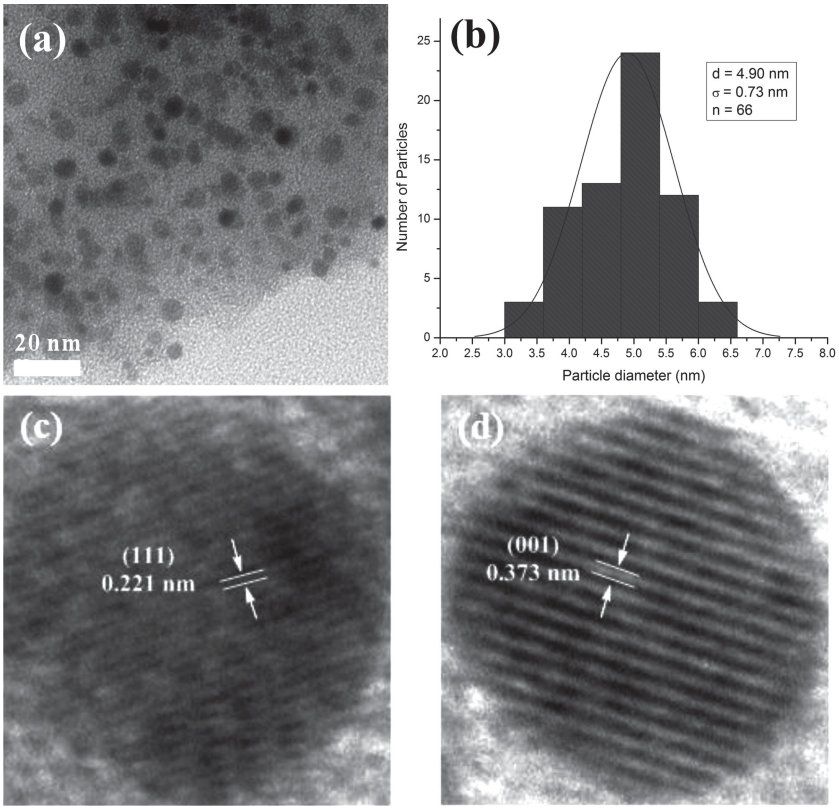

Figure 2. a) TEM characterization of FePt NPs synthesized through the direct pyrolysis of metallopolymer blend of $\mathbf{P}_{Fe}$ and $\mathbf{P}_{Pt}$ at 800 °C for 1 h under Ar. b) A particle-size histogram as measured from the TEM image in (a). c,d) High resolution TEM images of a single FePt NP.

homopolymers, we know that the resulting NPs are ferromagnetic $L1_0$-FePt alloy NPs. Thus, it convinces us that this method can be used as an alternative method for the facile preparation of nanopatterned array of $L1_0$-FePt NPs through NIL. Here, we use the soft PDMS nanodot mold with the periodicity and feature size of 500 nm and 250 nm, respectively, to imprint the polymer blend. **Figure 3** shows the SEM image of a nanoimprinted dot array pattern of the Fe-containing and Pt-containing metallopolymer blend. We can see that the negative pattern of the stamp was transferred onto the surface of polymer blend with high shape fidelity and conformity after nanoimprinting.

The orderly nanopatterned polymer blend was then allowed to anneal at 800 °C for 10 min under an argon atmosphere. After pyrolysis, a DC magnetic field of 1 T was applied in the out-of-plane direction to magnetize the sample. The topography of the annealed pattern was characterized by atomic force microscopy (AFM) (see **Figure 4**a: top view). Figure 4b shows the 3D topographical image of the dot array pattern of $L1_0$-FePt alloy NPs. The dot array structural patterns were preserved with the same pre-defined periodicity on the sample as indicated in Figure 3. The magnetic force microscopy (MFM) image of the nanopatterned dot array of $L1_0$-FePt NPs (see Figure 4c: top view) were taken in the interleave mode, by which only the magnetic signal (without the influence of topographical information) was acquired. Figure 4d shows the corresponding 3D MFM image. A dot array nanopattern of magnetization with the same periodicity as the dot array pattern in the corresponding AFM image (Figure 4a) can be observed clearly, which also indicates that this dot array nanopattern is magnetic and thereby can be used as a new platform for future perpendicular ultrahigh density magnetic data recording. The magnetic property of the nanodot

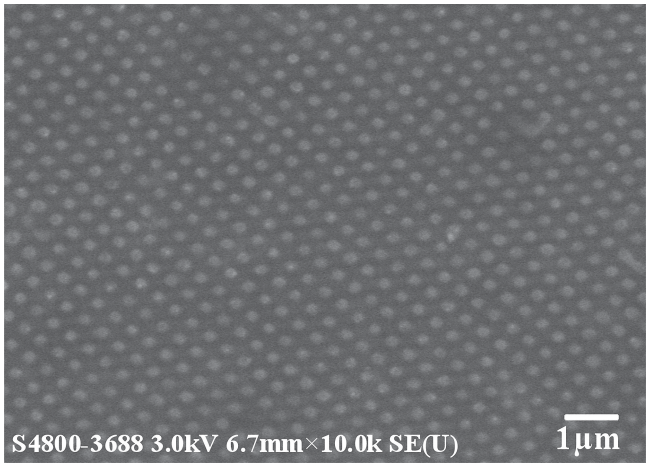

Figure 3. SEM image of the nanoimprinted dot array pattern of metallopolymer blend. The pattern periodicity and the feature size are approximately 500 nm and 250 nm, respectively.

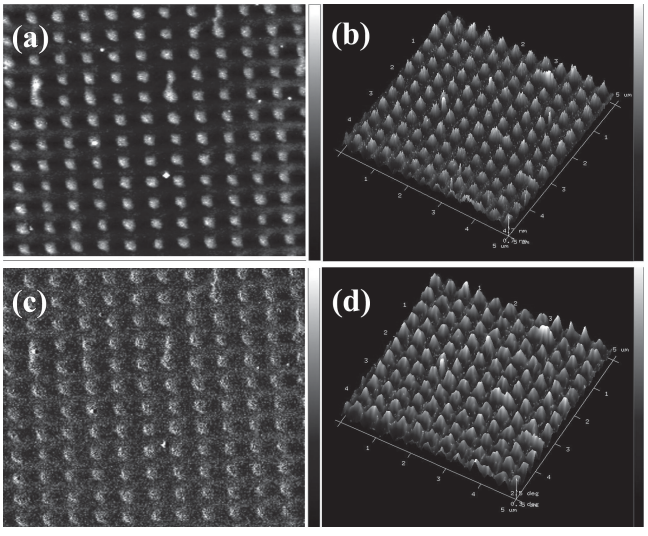

Figure 4. a) AFM image and c) MFM image of the nanoimprinted dot array pattern of FePt NPs with a periodicity of approximately 500 nm and the feature size of around 250 nm (top view). b) 3D AFM image and d) 3D MFM image showing the topography and magnetic morphology of the nanoimprinted dot array pattern, respectively.

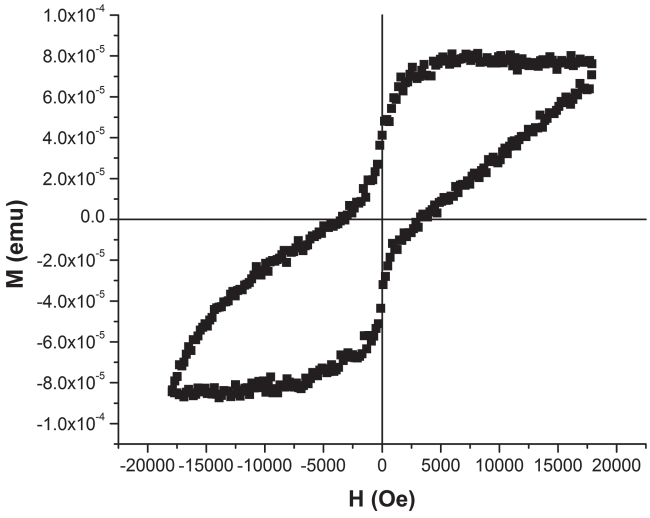

Figure 5. Hysteresis loop measurement by VSM at room temperature for the nanoimprinted dot array pattern of FePt NPs after pyrolysis.

patterned $L1_0$-FePt NPs was also characterized by vibrating sample magnetometer (VSM). The hysteresis loop measured at room temperature is shown in **Figure 5**, indicating that the coercivity of the dot array pattern of $L1_0$-FePt NPs was close to 0.38 T at room temperature, although the coercivity is low as compared with some literature values (2.23 T as measured by Lukehart et al. in 2006,[25] 1.4 T as measured by our group in 2012[16]), it is still suitable for practical application in data storage system, because information is easy to manipulate by an external magnetic field with a magnetic field strength achievable in typical magnetic data storage systems.[26] Measurement of FePt NPs in free-standing powder form showed much lower coercivity (227 Oe), but given the random orientation of the particles with respect to the measurement field, the result is as expected.[27,28] The remanant magnetization is about 50% of the saturation magnetization, a value that is expected for non-interacting NPs,[21,29] possibly due to the presence of carbonaceous matrix. It should also be noted that saturation does not seem to have reached within the limit of applied field of the VSM system; similar results have been reported by Sort et al.,[21] which they attributed the observation to a wide distribution of anisotropy energy among the NPs. Further magnetic analysis is needed to identify the exact origin of the exceedingly high saturation field in our samples.

3. Conclusions

We reported the synthesis of two Fe-containing and Pt-containing metallopolymers which exhibited excellent solubility in common organic solvents. $L1_0$ phase FePt NPs can be synthesized in one-step through controlled pyrolysis of the metallopolymer blend consisting of each of these monometallic Fe-containing and Pt-containing homopolymers. In addition, the excellent solubility and film-forming ability of these metallopolymers allowed the feasibility of patterning the polymer blend by nanoimprint lithography. Then, by pyrolytic treatment of the nanopatterned dot array of the polymer blend, a corresponding dot array pattern of $L1_0$-FePt NPs was generated directly with high conformity and shape fidelity of the original mold. MFM and VSM measurements proved that the resulting nanopatterned $L1_0$-FePt dot arrays were magnetic with a coercivity of 0.38 T. This suggests that the blending-patterning-pyrolysis approach we described here has great promise as a new platform for next generation perpendicular magnetic data recording based on nanopatterned $L1_0$-FePt NP-based BPM.

4. Experimental Section

General Procedures and Materials: All reactions were carried out under nitrogen unless otherwise stated. Commercially available reagents were used as received without further purification. All reactions were monitored by thin-layer chromatography (TLC) with Merck pre-coated glass plates. Compounds were visualized with UV light irradiation at 254 and 365 nm. Separation or purification of products was achieved by column chromatography or preparative TLC using silica gel from Merck (230–400 mesh). NMR spectra were measured in $CDCl_3$ on a JEOL JNM-EX270 FT NMR system or Bruker AV 400 NMR instrument with chemical shifts being referenced against tetramethylsilane as the internal standard for ^1H and ^{13}C NMR data. IR spectra were recorded on the Nicolet Magna 550 Series II FTIR spectrometer using KBr pellets for solid state spectroscopy. The positive-ion fast atom bombardment (FAB) mass spectra were recorded in *m*-nitrobenzyl alcohol matrix on a Finnigan-MAT SSQ710 mass spectrometer. Thermal analyses were performed with a Perkin-Elmer TGA 6 thermal analyzer. The molecular weight of the polymer was determined by Gel Permeation Chromatography (GPC) using a HP 1050 series HPLC instrument with visible wavelength and fluorescent detectors against polystyrene standards.

Nanoparticle Characterization: Structural characterization of the as-synthesized FePt NPs was performed by PXRD on a JEOL-3530 machine, with Cu$K\alpha_1$ (λ = 1.541 Å, 40 kV, 30 mA), for analyzing the composition and phase purity of the resulting NPs. TEM was performed on a Philips Tecnai G2 20 S-TWIN for probing the morphology, particle size and size distribution of NPs, and EDX spectra were done on a LEO 1530 scanning electron microscope for studying the ratio of Fe and Pt in the resulting metal alloy NPs. The morphology and magnetic properties of the as-prepared nanosized arrays of $L1_0$ phase FePt NPs were investigated by Digital Instruments NanoScope IV and Lakeshore 7400 series VSM system.

Synthesis of Fe-containing Metallopolymer: A mixture of 2,7-diethynyl-9-ferrocenylmethylenefluorene (52 mg, 0.127 mmol) and 2,7-diiodo-9,9-dihexadecylfluorene (110 mg, 0.127 mmol) was dissolved in NEt_3/THF (30 mL, 4:1 v/v), followed by the addition of CuI (10 mg) and $Pd(PPh_3)_4$ (15 mg). The red solution was stirred overnight under a nitrogen atmosphere at room temperature. The solvent was removed and the mixture was redissolved in a small amount of CH_2Cl_2. The solution was filtered and methanol (30 mL) was added into the filtrate to allow the precipitation of the polymer. The Fe-containing metallopolymer (P_{Fe}) was collected as a red solid (29.1 mg, 41%). ^1H NMR ($CDCl_3$, 400 MHz, δ/ppm): 7.71–7.69 (m, 1H, Ar-*H*), 7.67–7.66 (m, 4H, Ar-*H*), 7.56–7.51 (m, 4H, Ar-*H*), 7.30–7.26 (d, *J* = 16 Hz, 1H, C*H* = CH), 7.14–7.10 (d, *J* = 16 Hz, 1H, CH = C*H*), 4.57 (s, 2H, Fc-*H*), 4.36 (s, 2H, Fc-*H*), 4.21–4.19 (m, 5H, Fc-*H*), 2.04 (m, 4H, 9-fluorene-CH_2CH$_2$), 1.25–1.08 (m, 52H, CH_2), 0.87 (m, 6H, CH_2CH_3), 0.64 (m, 4H, $CH_2CH_2CH_3$); IR (KBr): 2207 ($\nu_{C\equiv C}$) cm^{-1}; Anal. Calc. for $(C_{67}H_{86}Fe)_n$: C, 84.95; H, 9.15; found: C, 84.83; H, 9.05%; GPC (THF): M_w = 74130, M_n = 19550, M_w/M_n = 3.79, DP = 20.

Synthesis of Pt-containing Metallopolymer: To a solution of 2,7-diethynyl-9,9-dihexadecylfluorene (155 mg, 0.234 mmol) in 30 mL of dichloromethane/triethylamine (1:1, v/v) was added $Pt(L)Cl_2$ (L = 4,4′-dinonyl-2,2′-bipyridyl) (158 mg, 0.234 mmol) and copper iodide (10 mg). The mixture was allowed to stir at room temperature

overnight under a nitrogen atmosphere. Afterwards the solvent was removed and the mixture was redissolved in a small amount of CH_2Cl_2 and reprecipitated with the addition of methanol. Centrifugation was performed to give a residual solid. The Pt-containing metallopolymer (P_{Pt}) was isolated as an orange-red solid (258 mg, 83%). ^{1}H NMR ($CDCl_3$, 400 MHz, δ/ppm): 9.81–9.58 (m, 2H, Ar-*H*), 8.01–7.58 (m, 10H, Ar-*H*), 2.79 (m, 4H, 9-fluorene-CH_2CH$_2$), 2.00–1.20 (m, 84H, CH_2), 0.84 (t, J = 20 Hz, 12H, CH$_2$CH_3), 0.56 (m, 4H, CH$_2$CH_2CH$_3$); IR (KBr): 2106.32 ($\upsilon_{C\equiv C}$) cm^{-1}; Anal. Calc. for $(C_{77}H_{116}N_2Pt)_n$: C, 73.12; H, 9.24; found: C, 73.20; H, 9.45%; GPC (THF): M_w = 12940, M_n = 9970, M_w/M_n = 1.30, DP = 8.

Pyrolytic Studies of Metallopolymer Blend: As-synthesized metallopolymers P_{Fe} and P_{Pt} with equiatomic ratio of Fe and Pt were mixed together in chloroform to form a saturated solution. Next, the polymer blend was put in a ceramic boat, which was then placed inside a quartz reaction tube equipped with temperature and gas-flow controls. Then, the whole set-up was heated up to 800 °C at a rate of 20 °C min^{-1}, and the polymer was allowed to pyrolyze at 800 °C for 1 h under an argon atmosphere.

Fabrication of Patterned $L1_0$-FePt NPs by NIL: Firstly, the Fe-containing and Pt-containing metallopolymers with equal atomic ratio of Fe and Pt were allowed to mix up sufficiently well in chloroform to form a saturated solution which was filtered. Secondly, the saturated solution of polymer blend in chloroform was drop-cast onto a silicon substrate which was previously rinsed in acetone followed by sonication in deionized water. Next, the soft PDMS nanodot mold was used to imprint patterns onto the silicon substrate with a constant and uniform force. During this step, the whole sample was exposed to ultraviolet radiation (25 mW cm^{-2}, 391 nm) for 5 min, which presumably cross-linked the metallopolymer and transformed the mixed polymer with low molecular weight into one with higher molecular weight. The solvent was also evaporated away in this step and left the mixed polymer in the solid phase. Then, the PDMS mask was lifted from the substrate surface and a negative copy of the pattern was replicated to the polymer blend on the sample surface. Finally, the sample was dry etched with reactive ion etching (RIE) to remove any residue in the trenches.

Supporting Information

Supporting Information is available from the Wiley Online Library or from the author.

Acknowledgements

Q. Dong and G. Li contributed equally to this work. We acknowledge the financial support from the National Natural Science Foundation of China (Grant No. 51373145 and No. 61307030), Hong Kong Research Grants Council (HKBU203312) and a FRG grant from Hong Kong Baptist University (FRG2/11–12/156). This work was also supported by the University Grants Committee Areas of Excellence Scheme (AoE/P-03/08). Support from the Seed Funding Program for Basic Research and Small Project Funding Program from the University of Hong Kong, ITF Tier 3 funding (ITS/112/12), RGC-GRF grant (HKU 704911P), University Grants Committee of Hong Kong (Contract No. AoE/P-04/08), and the Hong Kong Polytechnic University (A-PM21) was also acknowledged. W.-Y.W. and I.M. also thank financial support from the Royal Society International Exchanges Scheme (RS reference number IE110647).

Received: April 3, 2013
Revised: June 20, 2013
Published online: September 19, 2013

[1] S. Sun, C. B. Murray, D. Weller, L. Folks, A. Moser, *Science* **2000**, *27*, 1989.
[2] T. Thomson, S. L. Lee, M. F. Toney, C. D. Dewhurst, F. Y. Ogrin, C. J. Oates, S. Sun, *Phys. Rev. B* **2005**, *72*, 064441.
[3] H. L. Nguyen, L. E. M. Howard, G. W. Stinton, S. R. Giblin, B. K. Tanner, I. Terry, A. K. Hughes, I. M. Ross, A. Serres, J. S. O. Evans, *Chem. Mater.* **2006**, *18*, 6414.
[4] S. Sun, *Adv. Mater.* **2006**, *18*, 393.
[5] N. A. Frey, S. Peng, K. Cheng, S. Sun, *Chem. Soc. Rev.* **2009**, *38*, 2532.
[6] I. Robinson, S. Zacchini, L. D. Tung, S. Maenosono, N. T. K. Thanh, *Chem. Mater.* **2009**, *21*, 3021.
[7] A. Capobianchi, M. Colapietro, D. Fiorani, S. Foglia, P. Imperatori, S. Laureti, E. Palange, *Chem. Mater.* **2009**, *21*, 2007.
[8] L. Guo, *J. Adv. Mater.* **2007**, *19*, 495.
[9] Q. Guo, X. Teng, H. Yang, *Adv. Mater.* **2004**, *15*, 1337.
[10] X. Yang, Y. Xu, K. Lee, S. Xiao, D. S. Kuo, D. K. Weller, *IEEE Trans. Mag.* **2009**, *45*, 833.
[11] S. B. Clendenning, S. Aouba, M. S. Rayat, D. Grozea, J. B. Sorge, P. M. Brodersen, R. N. S. Sodhi, Z. H. Lu, C. M. Yip, M. R. Freeman, H. E. Reda, I. Manner, *Adv. Mater.* **2004**, *16*, 215.
[12] K. Liu, C. L. Ho, S. Aouba, Y. Q. Zhao, Z. H. Lu, S. Petrov, N. Coombs, P. Dube, H. E. Ruda, W. Y. Wong, I. Manners, *Angew. Chem. Int. Ed.* **2008**, *47*, 1255.
[13] K. Liu, S. Fournier-Bidoz, G. A. Ozin, I. Manners, *Chem. Mater.* **2009**, *21*, 1781.
[14] G. R. Whittell, M. D. Hager, U. S. Schubert, I. Manners, *Nat. Mater.* **2011**, *10*, 176.
[15] T. Ruotsalainen, J. Turku, P. Heikkilä, J. Ruokolainen, A. Nykänen, T. Laitinen, M. Torkkeli, R. Serimaa, G. Brinke, A. Harlin, O. Ikkala, *Adv. Mater.* **2005**, *17*, 1048.
[16] Q. Dong, G. Li, C. L. Ho, M. Faisal, C. W. Leung, P. W. T. Pong, K. Liu, B. Z. Tang, I. Manners, W. Y. Wong, *Adv. Mater.* **2012**, *24*, 1034.
[17] U. S. Schubert, C. Eschbaumer, *Angew. Chem. Int. Ed.* **2002**, *41*, 2892.
[18] I. Manners, *Synthetic Metal-Containing Polymers*, Wiley-VCH, Germany **2004**.
[19] K. A. Williams, A. J. Boydston, C. W. Bielawski, *Chem. Soc. Rev.* **2007**, *36*, 729.
[20] J. B. Gilroy, S. K. Patra, J. M. Mitchels, M. A. Winnik I. Manners, *Angew. Chem. Int. Ed.* **2011**, *50*, 5851.
[21] J. Sort, S. Suriñach, M. D. Baró, D. Muraviev, G. I. Dzhardimalieva, N. D. Golubeva, S. I. Pomogailo, A. D. Pomogailo, W. A. A. Macedo, D. Weller, V. Skumryev, J. Nogués, *Adv. Mater.* **2006**, *18*, 466.
[22] M. S. Wellons, W. H. Morris, Z. Gai, J. Shen, J. Bentley, J. E. Wittig, C. M. Lukehart, *Chem. Mater.* **2007**, *19*, 2483.
[23] J. P. Wang, *Proc. IEEE* **2008**, *96*, 1847.
[24] D. Weller, M. F. Doerner, *Ann. Rev. Mater. Sci.* **2000**, *30*, 611.
[25] R. D. Rutledge, W. H. Morris III, M. S. Wellons, Z. Gai, J. Shen, J. Bentley, J. E. Wittig, C. M. Lukehart, *J. Am. Chem. Soc.* **2006**, *128*, 14210.
[26] M. Schvartzman, S. J. Wind, *Nano Lett.* **2009**, *9*, 3629.
[27] K. Yano, V. Nandwanda, N. Poudyal, C. B. Rong, J. P. Liu, *J. Appl. Phys.* **2008**, *104*, 013918.
[28] B. D. Cullity, *Introduction to Magnetic Materials*, Addison-Wesley, Reading, USA **1972**.
[29] E. C. Stoner, E. P. Wohlfarth, *Philos. Trans. R. Soc. London, Ser. A* **1948**, *240*, 599.